April 2008
BABAR-PUB-08/011
SLAC-PUB-13197
arXiv:0804.2422 [hep-ex]

Observation of $B^+ \to \eta\rho^+$ and search for B^0 Decays to $\eta'\eta$, $\eta\pi^0$, $\eta'\pi^0$, and $\omega\pi^0$

B. Aubert,[1] M. Bona,[1] Y. Karyotakis,[1] J. P. Lees,[1] V. Poireau,[1] E. Prencipe,[1] X. Prudent,[1] V. Tisserand,[1] J. Garra Tico,[2] E. Grauges,[2] L. Lopez,[3] A. Palano,[3] M. Pappagallo,[3] G. Eigen,[4] B. Stugu,[4] L. Sun,[4] G. S. Abrams,[5] M. Battaglia,[5] D. N. Brown,[5] J. Button-Shafer,[5] R. N. Cahn,[5] R. G. Jacobsen,[5] J. A. Kadyk,[5] L. T. Kerth,[5] Yu. G. Kolomensky,[5] G. Kukartsev,[5] G. Lynch,[5] I. L. Osipenkov,[5] M. T. Ronan,[5,*] K. Tackmann,[5] T. Tanabe,[5] W. A. Wenzel,[5] C. M. Hawkes,[6] N. Soni,[6] A. T. Watson,[6] H. Koch,[7] T. Schroeder,[7] D. Walker,[8] D. J. Asgeirsson,[9] T. Cuhadar-Donszelmann,[9] B. G. Fulsom,[9] C. Hearty,[9] T. S. Mattison,[9] J. A. McKenna,[9] M. Barrett,[10] A. Khan,[10] M. Saleem,[10] L. Teodorescu,[10] V. E. Blinov,[11] A. D. Bukin,[11] A. R. Buzykaev,[11] V. P. Druzhinin,[11] V. B. Golubev,[11] A. P. Onuchin,[11] S. I. Serednyakov,[11] Yu. I. Skovpen,[11] E. P. Solodov,[11] K. Yu. Todyshev,[11] M. Bondioli,[12] S. Curry,[12] I. Eschrich,[12] D. Kirkby,[12] A. J. Lankford,[12] P. Lund,[12] M. Mandelkern,[12] E. C. Martin,[12] D. P. Stoker,[12] S. Abachi,[13] C. Buchanan,[13] J. W. Gary,[14] F. Liu,[14] O. Long,[14] B. C. Shen,[14,*] G. M. Vitug,[14] Z. Yasin,[14] L. Zhang,[14] V. Sharma,[15] C. Campagnari,[16] T. M. Hong,[16] D. Kovalskyi,[16] M. A. Mazur,[16] J. D. Richman,[16] T. W. Beck,[17] A. M. Eisner,[17] C. J. Flacco,[17] C. A. Heusch,[17] J. Kroseberg,[17] W. S. Lockman,[17] T. Schalk,[17] B. A. Schumm,[17] A. Seiden,[17] L. Wang,[17] M. G. Wilson,[17] L. O. Winstrom,[17] C. H. Cheng,[18] D. A. Doll,[18] B. Echenard,[18] F. Fang,[18] D. G. Hitlin,[18] I. Narsky,[18] T. Piatenko,[18] F. C. Porter,[18] R. Andreassen,[19] G. Mancinelli,[19] B. T. Meadows,[19] K. Mishra,[19] M. D. Sokoloff,[19] F. Blanc,[20] P. C. Bloom,[20] W. T. Ford,[20] A. Gaz,[20] J. D. Gilman,[20] J. Hachtel,[20] J. F. Hirschauer,[20] A. Kreisel,[20] M. Nagel,[20] U. Nauenberg,[20] A. Olivas,[20] J. G. Smith,[20] K. A. Ulmer,[20] S. R. Wagner,[20] C. G. West,[20] R. Ayad,[21,†] A. M. Gabareen,[21] A. Soffer,[21,‡] W. H. Toki,[21] R. J. Wilson,[21] D. D. Altenburg,[22] E. Feltresi,[22] A. Hauke,[22] H. Jasper,[22] M. Karbach,[22] J. Merkel,[22] A. Petzold,[22] B. Spaan,[22] K. Wacker,[22] V. Klose,[23] M. J. Kobel,[23] H. M. Lacker,[23] W. F. Mader,[23] R. Nogowski,[23] K. R. Schubert,[23] R. Schwierz,[23] J. E. Sundermann,[23] A. Volk,[23] D. Bernard,[24] G. R. Bonneaud,[24] E. Latour,[24] Ch. Thiebaux,[24] M. Verderi,[24] P. J. Clark,[25] W. Gradl,[25] S. Playfer,[25] J. E. Watson,[25] M. Andreotti,[26] D. Bettoni,[26] C. Bozzi,[26] R. Calabrese,[26] A. Cecchi,[26] G. Cibinetto,[26] P. Franchini,[26] E. Luppi,[26] M. Negrini,[26] A. Petrella,[26] L. Piemontese,[26] V. Santoro,[26] F. Anulli,[27] R. Baldini-Ferroli,[27] A. Calcaterra,[27] R. de Sangro,[27] G. Finocchiaro,[27] S. Pacetti,[27] P. Patteri,[27] I. M. Peruzzi,[27,§] M. Piccolo,[27] M. Rama,[27] A. Zallo,[27] A. Buzzo,[28] R. Contri,[28] M. Lo Vetere,[28] M. M. Macri,[28] M. R. Monge,[28] S. Passaggio,[28] C. Patrignani,[28] E. Robutti,[28] A. Santroni,[28] S. Tosi,[28] K. S. Chaisanguanthum,[29] M. Morii,[29] R. S. Dubitzky,[30] J. Marks,[30] S. Schenk,[30] U. Uwer,[30] D. J. Bard,[31] P. D. Dauncey,[31] J. A. Nash,[31] W. Panduro Vazquez,[31] M. Tibbetts,[31] P. K. Behera,[32] X. Chai,[32] M. J. Charles,[32] U. Mallik,[32] J. Cochran,[33] H. B. Crawley,[33] L. Dong,[33] W. T. Meyer,[33] S. Prell,[33] E. I. Rosenberg,[33] A. E. Rubin,[33] Y. Y. Gao,[34] A. V. Gritsan,[34] Z. J. Guo,[34] C. K. Lae,[34] A. G. Denig,[35] M. Fritsch,[35] G. Schott,[35] N. Arnaud,[36] J. Béquilleux,[36] A. D'Orazio,[36] M. Davier,[36] J. Firmino da Costa,[36] G. Grosdidier,[36] A. Höcker,[36] V. Lepeltier,[36] F. Le Diberder,[36] A. M. Lutz,[36] S. Pruvot,[36] P. Roudeau,[36] M. H. Schune,[36] J. Serrano,[36] V. Sordini,[36] A. Stocchi,[36] W. F. Wang,[36] G. Wormser,[36] D. J. Lange,[37] D. M. Wright,[37] I. Bingham,[38] J. P. Burke,[38] C. A. Chavez,[38] J. R. Fry,[38] E. Gabathuler,[38] R. Gamet,[38] D. E. Hutchcroft,[38] D. J. Payne,[38] C. Touramanis,[38] A. J. Bevan,[39] K. A. George,[39] F. Di Lodovico,[39] R. Sacco,[39] M. Sigamani,[39] G. Cowan,[40] H. U. Flaecher,[40] D. A. Hopkins,[40] S. Paramesvaran,[40] F. Salvatore,[40] A. C. Wren,[40] D. N. Brown,[41] C. L. Davis,[41] K. E. Alwyn,[42] N. R. Barlow,[42] R. J. Barlow,[42] Y. M. Chia,[42] C. L. Edgar,[42] G. D. Lafferty,[42] T. J. West,[42] J. I. Yi,[42] J. Anderson,[43] C. Chen,[43] A. Jawahery,[43] D. A. Roberts,[43] G. Simi,[43] J. M. Tuggle,[43] C. Dallapiccola,[44] S. S. Hertzbach,[44] X. Li,[44] E. Salvati,[44] S. Saremi,[44] R. Cowan,[45] D. Dujmic,[45] P. H. Fisher,[45] K. Koeneke,[45] G. Sciolla,[45] M. Spitznagel,[45] F. Taylor,[45] R. K. Yamamoto,[45] M. Zhao,[45] S. E. Mclachlin,[46,*] P. M. Patel,[46] S. H. Robertson,[46] A. Lazzaro,[47] V. Lombardo,[47] F. Palombo,[47] J. M. Bauer,[48] L. Cremaldi,[48] V. Eschenburg,[48] R. Godang,[48] R. Kroeger,[48] D. A. Sanders,[48] D. J. Summers,[48] H. W. Zhao,[48] S. Brunet,[49] D. Côté,[49] M. Simard,[49] P. Taras,[49] F. B. Viaud,[49] H. Nicholson,[50] G. De Nardo,[51] L. Lista,[51] D. Monorchio,[51] C. Sciacca,[51] M. A. Baak,[52] G. Raven,[52] H. L. Snoek,[52] C. P. Jessop,[53] K. J. Knoepfel,[53] J. M. LoSecco,[53] G. Benelli,[54] L. A. Corwin,[54] K. Honscheid,[54] H. Kagan,[54] R. Kass,[54] J. P. Morris,[54] A. M. Rahimi,[54] J. J. Regensburger,[54] S. J. Sekula,[54] Q. K. Wong,[54] N. L. Blount,[55] J. Brau,[55] R. Frey,[55] O. Igonkina,[55] J. A. Kolb,[55] M. Lu,[55] R. Rahmat,[55]

Submitted to Physical Review D RC

Work supported in part by US Department of Energy contract DE-AC02-76SF00515

N. B. Sinev,[55] D. Strom,[55] J. Strube,[55] E. Torrence,[55] G. Castelli,[56] N. Gagliardi,[56] M. Margoni,[56] M. Morandin,[56]
M. Posocco,[56] M. Rotondo,[56] F. Simonetto,[56] R. Stroili,[56] C. Voci,[56] P. del Amo Sanchez,[57] E. Ben-Haim,[57]
H. Briand,[57] G. Calderini,[57] J. Chauveau,[57] P. David,[57] L. Del Buono,[57] O. Hamon,[57] Ph. Leruste,[57] J. Ocariz,[57]
A. Perez,[57] J. Prendki,[57] L. Gladney,[58] M. Biasini,[59] R. Covarelli,[59] E. Manoni,[59] C. Angelini,[60] G. Batignani,[60]
S. Bettarini,[60] M. Carpinelli,[60,¶] A. Cervelli,[60] F. Forti,[60] M. A. Giorgi,[60] A. Lusiani,[60] G. Marchiori,[60]
M. Morganti,[60] N. Neri,[60] E. Paoloni,[60] G. Rizzo,[60] J. J. Walsh,[60] J. Biesiada,[61] D. Lopes Pegna,[61] C. Lu,[61]
J. Olsen,[61] A. J. S. Smith,[61] A. V. Telnov,[61] E. Baracchini,[62] G. Cavoto,[62] D. del Re,[62] E. Di Marco,[62] R. Faccini,[62]
F. Ferrarotto,[62] F. Ferroni,[62] M. Gaspero,[62] P. D. Jackson,[62] L. Li Gioi,[62] M. A. Mazzoni,[62] S. Morganti,[62]
G. Piredda,[62] F. Polci,[62] F. Renga,[62] C. Voena,[62] M. Ebert,[63] T. Hartmann,[63] H. Schröder,[63] R. Waldi,[63]
T. Adye,[64] B. Franek,[64] E. O. Olaiya,[64] W. Roethel,[64] F. F. Wilson,[64] S. Emery,[65] M. Escalier,[65] L. Esteve,[65]
A. Gaidot,[65] S. F. Ganzhur,[65] G. Hamel de Monchenault,[65] W. Kozanecki,[65] G. Vasseur,[65] Ch. Yèche,[65] M. Zito,[65]
X. R. Chen,[66] H. Liu,[66] W. Park,[66] M. V. Purohit,[66] R. M. White,[66] J. R. Wilson,[66] M. T. Allen,[67] D. Aston,[67]
R. Bartoldus,[67] P. Bechtle,[67] J. F. Benitez,[67] R. Cenci,[67] J. P. Coleman,[67] M. R. Convery,[67] J. C. Dingfelder,[67]
J. Dorfan,[67] G. P. Dubois-Felsmann,[67] W. Dunwoodie,[67] R. C. Field,[67] S. J. Gowdy,[67] M. T. Graham,[67]
P. Grenier,[67] C. Hast,[67] W. R. Innes,[67] J. Kaminski,[67] M. H. Kelsey,[67] H. Kim,[67] P. Kim,[67] M. L. Kocian,[67]
D. W. G. S. Leith,[67] S. Li,[67] B. Lindquist,[67] S. Luitz,[67] V. Luth,[67] H. L. Lynch,[67] D. B. MacFarlane,[67]
H. Marsiske,[67] R. Messner,[67] D. R. Muller,[67] H. Neal,[67] S. Nelson,[67] C. P. O'Grady,[67] I. Ofte,[67] A. Perazzo,[67]
M. Perl,[67] B. N. Ratcliff,[67] A. Roodman,[67] A. A. Salnikov,[67] R. H. Schindler,[67] J. Schwiening,[67] A. Snyder,[67]
D. Su,[67] M. K. Sullivan,[67] K. Suzuki,[67] S. K. Swain,[67] J. M. Thompson,[67] J. Va'vra,[67] A. P. Wagner,[67]
M. Weaver,[67] C. A. West,[67] W. J. Wisniewski,[67] M. Wittgen,[67] D. H. Wright,[67] H. W. Wulsin,[67] A. K. Yarritu,[67]
K. Yi,[67] C. C. Young,[67] V. Ziegler,[67] P. R. Burchat,[68] A. J. Edwards,[68] S. A. Majewski,[68] T. S. Miyashita,[68]
B. A. Petersen,[68] L. Wilden,[68] S. Ahmed,[69] M. S. Alam,[69] R. Bula,[69] J. A. Ernst,[69] B. Pan,[69] M. A. Saeed,[69]
S. B. Zain,[69] S. M. Spanier,[70] B. J. Wogsland,[70] R. Eckmann,[71] J. L. Ritchie,[71] A. M. Ruland,[71] C. J. Schilling,[71]
R. F. Schwitters,[71] B. W. Drummond,[72] J. M. Izen,[72] X. C. Lou,[72] S. Ye,[72] F. Bianchi,[73] D. Gamba,[73]
M. Pelliccioni,[73] M. Bomben,[74] L. Bosisio,[74] C. Cartaro,[74] G. Della Ricca,[74] L. Lanceri,[74] L. Vitale,[74] V. Azzolini,[75]
N. Lopez-March,[75] F. Martinez-Vidal,[75] D. A. Milanes,[75] A. Oyanguren,[75] J. Albert,[76] Sw. Banerjee,[76]
B. Bhuyan,[76] H. H. F. Choi,[76] K. Hamano,[76] R. Kowalewski,[76] M. J. Lewczuk,[76] I. M. Nugent,[76] J. M. Roney,[76]
R. J. Sobie,[76] T. J. Gershon,[77] P. F. Harrison,[77] J. Ilic,[77] T. E. Latham,[77] G. B. Mohanty,[77] H. R. Band,[78]
X. Chen,[78] S. Dasu,[78] K. T. Flood,[78] Y. Pan,[78] M. Pierini,[78] R. Prepost,[78] C. O. Vuosalo,[78] and S. L. Wu[78]
(The *BABAR* Collaboration)

[1]*Laboratoire de Physique des Particules, IN2P3/CNRS et Université de Savoie, F-74941 Annecy-Le-Vieux, France*
[2]*Universitat de Barcelona, Facultat de Fisica, Departament ECM, E-08028 Barcelona, Spain*
[3]*Università di Bari, Dipartimento di Fisica and INFN, I-70126 Bari, Italy*
[4]*University of Bergen, Institute of Physics, N-5007 Bergen, Norway*
[5]*Lawrence Berkeley National Laboratory and University of California, Berkeley, California 94720, USA*
[6]*University of Birmingham, Birmingham, B15 2TT, United Kingdom*
[7]*Ruhr Universität Bochum, Institut für Experimentalphysik 1, D-44780 Bochum, Germany*
[8]*University of Bristol, Bristol BS8 1TL, United Kingdom*
[9]*University of British Columbia, Vancouver, British Columbia, Canada V6T 1Z1*
[10]*Brunel University, Uxbridge, Middlesex UB8 3PH, United Kingdom*
[11]*Budker Institute of Nuclear Physics, Novosibirsk 630090, Russia*
[12]*University of California at Irvine, Irvine, California 92697, USA*
[13]*University of California at Los Angeles, Los Angeles, California 90024, USA*
[14]*University of California at Riverside, Riverside, California 92521, USA*
[15]*University of California at San Diego, La Jolla, California 92093, USA*
[16]*University of California at Santa Barbara, Santa Barbara, California 93106, USA*
[17]*University of California at Santa Cruz, Institute for Particle Physics, Santa Cruz, California 95064, USA*
[18]*California Institute of Technology, Pasadena, California 91125, USA*
[19]*University of Cincinnati, Cincinnati, Ohio 45221, USA*
[20]*University of Colorado, Boulder, Colorado 80309, USA*
[21]*Colorado State University, Fort Collins, Colorado 80523, USA*
[22]*Technische Universität Dortmund, Fakultät Physik, D-44221 Dortmund, Germany*
[23]*Technische Universität Dresden, Institut für Kern- und Teilchenphysik, D-01062 Dresden, Germany*
[24]*Laboratoire Leprince-Ringuet, CNRS/IN2P3, Ecole Polytechnique, F-91128 Palaiseau, France*
[25]*University of Edinburgh, Edinburgh EH9 3JZ, United Kingdom*
[26]*Università di Ferrara, Dipartimento di Fisica and INFN, I-44100 Ferrara, Italy*

[27]*Laboratori Nazionali di Frascati dell'INFN, I-00044 Frascati, Italy*
[28]*Università di Genova, Dipartimento di Fisica and INFN, I-16146 Genova, Italy*
[29]*Harvard University, Cambridge, Massachusetts 02138, USA*
[30]*Universität Heidelberg, Physikalisches Institut, Philosophenweg 12, D-69120 Heidelberg, Germany*
[31]*Imperial College London, London, SW7 2AZ, United Kingdom*
[32]*University of Iowa, Iowa City, Iowa 52242, USA*
[33]*Iowa State University, Ames, Iowa 50011-3160, USA*
[34]*Johns Hopkins University, Baltimore, Maryland 21218, USA*
[35]*Universität Karlsruhe, Institut für Experimentelle Kernphysik, D-76021 Karlsruhe, Germany*
[36]*Laboratoire de l'Accélérateur Linéaire, IN2P3/CNRS et Université Paris-Sud 11,*
Centre Scientifique d'Orsay, B. P. 34, F-91898 ORSAY Cedex, France
[37]*Lawrence Livermore National Laboratory, Livermore, California 94550, USA*
[38]*University of Liverpool, Liverpool L69 7ZE, United Kingdom*
[39]*Queen Mary, University of London, E1 4NS, United Kingdom*
[40]*University of London, Royal Holloway and Bedford New College, Egham, Surrey TW20 0EX, United Kingdom*
[41]*University of Louisville, Louisville, Kentucky 40292, USA*
[42]*University of Manchester, Manchester M13 9PL, United Kingdom*
[43]*University of Maryland, College Park, Maryland 20742, USA*
[44]*University of Massachusetts, Amherst, Massachusetts 01003, USA*
[45]*Massachusetts Institute of Technology, Laboratory for Nuclear Science, Cambridge, Massachusetts 02139, USA*
[46]*McGill University, Montréal, Québec, Canada H3A 2T8*
[47]*Università di Milano, Dipartimento di Fisica and INFN, I-20133 Milano, Italy*
[48]*University of Mississippi, University, Mississippi 38677, USA*
[49]*Université de Montréal, Physique des Particules, Montréal, Québec, Canada H3C 3J7*
[50]*Mount Holyoke College, South Hadley, Massachusetts 01075, USA*
[51]*Università di Napoli Federico II, Dipartimento di Scienze Fisiche and INFN, I-80126, Napoli, Italy*
[52]*NIKHEF, National Institute for Nuclear Physics and High Energy Physics, NL-1009 DB Amsterdam, The Netherlands*
[53]*University of Notre Dame, Notre Dame, Indiana 46556, USA*
[54]*Ohio State University, Columbus, Ohio 43210, USA*
[55]*University of Oregon, Eugene, Oregon 97403, USA*
[56]*Università di Padova, Dipartimento di Fisica and INFN, I-35131 Padova, Italy*
[57]*Laboratoire de Physique Nucléaire et de Hautes Energies,*
IN2P3/CNRS, Université Pierre et Marie Curie-Paris6,
Université Denis Diderot-Paris7, F-75252 Paris, France
[58]*University of Pennsylvania, Philadelphia, Pennsylvania 19104, USA*
[59]*Università di Perugia, Dipartimento di Fisica and INFN, I-06100 Perugia, Italy*
[60]*Università di Pisa, Dipartimento di Fisica, Scuola Normale Superiore and INFN, I-56127 Pisa, Italy*
[61]*Princeton University, Princeton, New Jersey 08544, USA*
[62]*Università di Roma La Sapienza, Dipartimento di Fisica and INFN, I-00185 Roma, Italy*
[63]*Universität Rostock, D-18051 Rostock, Germany*
[64]*Rutherford Appleton Laboratory, Chilton, Didcot, Oxon, OX11 0QX, United Kingdom*
[65]*DSM/Dapnia, CEA/Saclay, F-91191 Gif-sur-Yvette, France*
[66]*University of South Carolina, Columbia, South Carolina 29208, USA*
[67]*Stanford Linear Accelerator Center, Stanford, California 94309, USA*
[68]*Stanford University, Stanford, California 94305-4060, USA*
[69]*State University of New York, Albany, New York 12222, USA*
[70]*University of Tennessee, Knoxville, Tennessee 37996, USA*
[71]*University of Texas at Austin, Austin, Texas 78712, USA*
[72]*University of Texas at Dallas, Richardson, Texas 75083, USA*
[73]*Università di Torino, Dipartimento di Fisica Sperimentale and INFN, I-10125 Torino, Italy*
[74]*Università di Trieste, Dipartimento di Fisica and INFN, I-34127 Trieste, Italy*
[75]*IFIC, Universitat de Valencia-CSIC, E-46071 Valencia, Spain*
[76]*University of Victoria, Victoria, British Columbia, Canada V8W 3P6*
[77]*Department of Physics, University of Warwick, Coventry CV4 7AL, United Kingdom*
[78]*University of Wisconsin, Madison, Wisconsin 53706, USA*

(Dated: April 15, 2008)

We present measurements of branching fractions for five B-meson decays to two-body charmless final states. The data, collected with the *BABAR* detector at the Stanford Linear Accelerator Center, represent 459 million $B\overline{B}$ pairs. The results for branching fractions are, in units of 10^{-6} (upper limits at 90% C.L.): $\mathcal{B}(B^+ \rightarrow \eta\rho^+) = 9.9 \pm 1.2 \pm 0.8$, $\mathcal{B}(B^0 \rightarrow \eta'\eta) = 0.5 \pm 0.4 \pm 0.1$ (< 1.2), $\mathcal{B}(B^0 \rightarrow \eta\pi^0) = 0.9 \pm 0.4 \pm 0.1$ (< 1.5), $\mathcal{B}(B^0 \rightarrow \eta'\pi^0) = 0.9 \pm 0.4 \pm 0.1$ (< 1.5), and $\mathcal{B}(B^0 \rightarrow \omega\pi^0) = 0.07 \pm 0.26 \pm 0.02$ (< 0.5). The first error quoted is statistical and the second systematic. For the $\eta\rho^+$ mode, we measure the charge asymmetry $\mathcal{A}_{ch}(B^+ \rightarrow \eta\rho^+) = 0.13 \pm 0.11 \pm 0.02$.

PACS numbers: 13.25.Hw, 12.15.Hh, 11.30.Er

Measurements of charmless B decays are now routinely used to test the accuracy of theoretical predictions based on, for example, QCD factorization [1, 2], flavor SU(3) symmetry [3–5], perturbative QCD [6], or soft collinear effective theory [7]. We present measurements of the branching fraction and charge asymmetry for the decay $B^+ \to \eta\rho^+$ (charge conjugate reactions are implied throughout this paper), superseding our previous result that found a 4.7σ signal for this decay [8] with a luminosity of about one-half that used in this paper. In addition we search for the decays $B^0 \to \eta'\eta$, $B^0 \to \eta\pi^0$, $B^0 \to \eta'\pi^0$, and $B^0 \to \omega\pi^0$. None of these decays have been observed previously though limits have been reported by *BABAR* [9], Belle [10], and CLEO [11].

In the Standard Model (SM) the dominant processes that contribute to these decays are described by tree amplitudes and to a lesser extent penguin (loop) amplitudes. For $B^0 \to \eta'\pi^0$ and $B^0 \to \eta\pi^0$ the color-suppressed tree diagram is suppressed by approximate cancellation between the amplitudes for the π^0 and for the isoscalar meson that contains the spectator quark. The approximate ranges of expectations [1–7] for the branching fraction are $\sim 10\times10^{-6}$ for $B^+ \to \eta\rho^+$, 0.3–2×10^{-6} for $B^0 \to \eta'\eta$, 0.2–1.0×10^{-6} for $B^0 \to \eta^{(\prime)}\pi^0$, and $\sim 0.1\times10^{-6}$ for $B^0 \to \omega\pi^0$. Direct *CP* violation could be detected as a charge asymmetry, defined as $\mathcal{A}_{ch} \equiv (\Gamma^- - \Gamma^+)/(\Gamma^- + \Gamma^+)$, where the superscript on the width Γ corresponds to the sign of the $B^\pm$ meson; $\mathcal{A}_{ch}$ for $B^+ \to \eta\rho^+$ is expected to be small since the decay is dominated by a single amplitude.

These B^0 decays are also of interest in constraining the expected value of the time-dependent *CP*-violation asymmetry parameter S_f in the B decay with final state $f = \eta' K^0_S$ [5, 12, 13]. The leading-order SM calculation gives the equality $S_{\eta' K^0_S} = S_{J/\psi K^0_S}$, where the latter has been precisely measured [14], and equals sin2β in the SM. The *CP* asymmetries in the charmless B decays are not only sensitive to contributions from new physics, but also to contamination from sub-leading SM amplitudes. Recent theoretical calculations of the size of the change in $S_{\eta' K^0_S}$ from these sub-leading amplitudes finds no more than 0.03 [7, 15]. The most stringent constraint from data on such contamination uses SU(3) and the measured branching fractions of the decays $B^0 \to \eta'\eta$, $B^0 \to \eta\pi^0$, $B^0 \to \eta'\pi^0$ [5, 12, 13]. Recently it has also been suggested [16, 17] that $B^0 \to \eta'\pi^0$ and $B^0 \to \eta\pi^0$ can be used to constrain the contribution from isospin-breaking effects on the value of sin2α in $B \to \pi^+\pi^-$ decays.

The results presented here are based on data collected with the *BABAR* detector [18] at the PEP-II asymmetric e^+e^- collider located at the Stanford Linear Accelerator Center. We recorded a data sample at the $\Upsilon(4S)$ resonance (center-of-mass energy $\sqrt{s} = 10.58$ GeV) with an integrated luminosity of 418 fb^{-1}, corresponding to $(459 \pm 5) \times 10^6$ $B\overline{B}$ pairs.

Charged particles from the e^+e^- interactions are detected and their momenta measured by a combination of five layers of double-sided silicon microstrip detectors and a 40-layer drift chamber, both operating in the 1.5 T magnetic field of a superconducting solenoid. Photons and electrons are identified with a CsI(Tl) electromagnetic calorimeter (EMC). Further charged particle identification (PID) is provided by the average energy loss (dE/dx) in the tracking devices and by an internally reflecting ring imaging Cherenkov detector (DIRC) covering the central region.

We establish the event selection criteria with the aid of a detailed Monte Carlo (MC) simulation of the B production and decay sequences, and of the detector response [19]. These criteria are designed to retain signal events with high efficiency. Applied to the data, they result in a sample much larger than the expected signal, but with well characterized backgrounds. We extract the signal yields from this sample with a maximum likelihood (ML) fit.

The B-daughter candidates are reconstructed through their decays $\pi^0 \to \gamma\gamma$, $\eta \to \gamma\gamma$ ($\eta_{\gamma\gamma}$), $\eta \to \pi^+\pi^-\pi^0$ ($\eta_{3\pi}$), $\eta' \to \eta_{\gamma\gamma}\pi^+\pi^-$ ($\eta'_{\eta\pi\pi}$), $\eta' \to \rho^0\gamma$ ($\eta'_{\rho\gamma}$), $\omega \to \pi^+\pi^-\pi^0$, $\rho^0 \to \pi^+\pi^-$ and $\rho^+ \to \pi^+\pi^0$. Table I lists the requirements on the invariant masses of these particles' final states. All requirements are kept loose ($> 3\sigma$) for later fitting except for the π^0 invariant mass which is not included in the fits. Secondary charged pions in η, η', and ω candidates are rejected if classified as protons, kaons, or electrons by a combination of their DIRC, dE/dx, and EMC PID signatures.

TABLE I: Selection requirements on the invariant masses of resonances and the laboratory energies of photons from their decay.

State	Invariant mass (MeV)	$E(\gamma)$ (MeV)
Prompt π^0	$120 < m(\gamma\gamma) < 150$	> 50
$\eta_{\gamma\gamma}$	$490 < m(\gamma\gamma) < 600$	> 100
$\eta_{3\pi}$	$520 < m(\pi^+\pi^-\pi^0) < 570$	> 30
$\eta'_{\eta\pi\pi}$	$910 < m(\pi^+\pi^-\eta) < 1000$	> 100
$\eta'_{\rho\gamma}$	$910 < m(\pi^+\pi^-\gamma) < 1000$	> 200
ω	$735 < m(\pi^+\pi^-\pi^0) < 825$	> 30
ρ^0	$510 < m(\pi^+\pi^-) < 1000$	—
ρ^+	$470 < m(\pi^+\pi^0) < 1070$	> 30

We reconstruct the B-meson candidate by combining the four-momenta of a pair of daughter mesons, with a vertex constraint if the ultimate final state includes at least two charged particles. Since the natural widths of the η, η', and π^0 mesons are much smaller than the resolution, we also constrain their masses to nominal values [20] in the fit of the B candidate. From the kinematics of the $\Upsilon(4S)$ decay we determine the energy-substituted mass $m_{\rm ES} = \sqrt{\frac{1}{4}s - \mathbf{p}_B^2}$ and the energy difference $\Delta E = E_B - \frac{1}{2}\sqrt{s}$, where $(E_B, \mathbf{p}_B)$ is the B-meson 4-momentum vector, and all values are expressed in the $\Upsilon(4S)$ rest frame. The resolution in $m_{\rm ES}$ is 3.0 MeV and in ΔE is 24–50 MeV, depending on the decay mode. We require 5.25 GeV $< m_{\rm ES} < 5.29$ GeV and $|\Delta E| < 0.25$ GeV (< 0.2 GeV for $B^0 \to \eta'\eta$ and $B^+ \to \eta\rho^+$).

Backgrounds arise primarily from random combinations of particles in continuum $e^+e^- \to q\overline{q}$ events ($q = u, d, s, c$). We reduce these with requirements on the angle $\theta_{\rm T}$ between the thrust axis of the B candidate's decay products in the $\Upsilon(4S)$ rest frame and the thrust axis of the rest of the charged tracks and neutral calorimeter clusters in the event. The distribution is sharply peaked near $|\cos\theta_{\rm T}| = 1$ for $q\overline{q}$ jet pairs and nearly uniform for B-meson decays. We require $|\cos\theta_{\rm T}| < 0.7$–$0.9$ depending on the decay mode.

In the ML fit we discriminate against $q\overline{q}$ background with a Fisher discriminant $\mathcal{F}$ that combines five variables [21]: the polar angles, with respect to the beam axis in the $\Upsilon(4S)$ rest frame, of the B candidate momentum and of the B thrust axis; the flavor tagging category [22]; and the zeroth and second angular moments of the energy flow, excluding the B candidate, about the B thrust axis. It provides about one standard deviation of separation between B decay events and combinatorial background.

We also impose restrictions on decay angles to exclude the most asymmetric decays where soft-particle backgrounds concentrate and the acceptance changes rapidly. We define the decay angle $\theta^k_{\rm dec}$ and its cosine $\mathcal{H}_k$ for a meson k as the angle between the momenta of a daughter particle and the meson's parent, measured in the meson's rest frame. We require for the $\eta'_{\rho\gamma}$ decays $|\mathcal{H}_{\rho^0}| < 0.9$ and for $\eta^{(\prime)}\pi^0$ $|\mathcal{H}_{\pi^0}| < 0.95$. For $B^0 \to \eta'_{\rho\gamma}\eta_{\gamma\gamma}$ we suppress the background $B \to K^*\gamma$ by requiring $|\mathcal{H}_\eta| < 0.86$. These distributions are uniform for signal except for $\mathcal{H}_{\rho^0}$ which has a $1 - \mathcal{H}_\rho^2$ distribution.

For the $B^+ \to \eta\rho^+$ decay, we define $\theta^k_{\rm dec}$ as the angle between the π^0 and the negative of the B momentum in the ρ rest frame. We require $-0.75 < \mathcal{H}_{\rho^+} < 0.95$. For the $B^0 \to \omega\pi^0$ decay, $|\mathcal{H}_\omega|$ is defined as the cosine of the angle between the normal to the ω decay plane (the plane of the three pions in the ω rest frame) and the flight direction of the B, measured in the ω rest frame. Both of these quantities have a $\mathcal{H}^2$ distribution for signal.

The average number of candidates found per selected event is in the range 1.06 to 1.47, depending on the final state. We choose the candidate with the largest probability for the fit to the B decay tree.

We obtain yields for each channel from a ML fit with the input observables ΔE, $m_{\rm ES}$, $\mathcal{F}$, m_k, $k = 1, 2$ (the daughter invariant mass spectrum of the η, η', ω, or ρ^+ candidate), and $\mathcal{H}_k$ the helicity of the ω or ρ^+ candidate. The selected sample sizes are given in the second column of Table II. Besides any signal events, the samples contain combinatorial background from $q\overline{q}$ (dominant) and $B\overline{B}$ with $b \to c$, and a component from other charmless $B\overline{B}$ modes that we estimate from the simulation to be no more than two percent of the sample. The latter events have ultimate final states different from the signal, but with similar kinematics so that broad peaks near those of the signal appear in some observables, requiring a separate component in the probability density function (PDF).

The likelihood function is

$$\mathcal{L} = \exp(-\sum_j Y_j)\prod_i^N \sum_j Y_j \times \tag{1}$$
$$\mathcal{P}_j({m_{\rm ES}}^i)\mathcal{P}_j(\Delta E^i)\mathcal{P}_j(\mathcal{F}^i)\mathcal{P}_j(m_1^i)\left[\mathcal{P}_j(m_2^i), \mathcal{P}_j(\mathcal{H}^i_{\omega,\rho^+})\right],$$

where N is the number of events in the sample, and, for each of the three components j, Y_j is the yield of events and $\mathcal{P}_j(x^i)$ the PDF for observable x in event i. For the mode $B^0 \to \eta'_{\eta\pi\pi}\eta_{3\pi}$ we found no need for the charmless $B\overline{B}$ background component. For the $B^+ \to \eta_{\gamma\gamma}\rho^+$ and $B^0 \to \omega\pi^0$ decays we split the charmless $B\overline{B}$ PDF into components made from backgrounds with and without a ρ^+. The factored form of the PDF indicated in Eq. 1 is appropriate since correlations among observables measured in the data are small. Distortions of the signal yields caused by this approximation are measured in simulation and included in the bias corrections and systematic errors discussed below.

We determine the PDFs for the signal and charmless $B\overline{B}$ background components from fits to MC simulated events. Large control samples of B decays to charmed final states of similar topology [$B^+ \to \overline{D}^0(K^+\pi^-\pi^0)\pi^+$ and $B^+ \to \overline{D}^0(K^+\pi^-\pi^0)\rho^+$] are used to verify the simulated resolutions in ΔE and $m_{\rm ES}$. Where the control data samples reveal small differences from MC, we shift or scale the resolution used in the ML fits. We develop PDFs for the combinatorial background with fits to the data from which the signal region (5.27 GeV $< m_{\rm ES} <$ 5.29 GeV and $|\Delta E| < 0.1$ GeV) has been excluded.

We use the following functional forms for the PDFs: sum of two Gaussians for $\mathcal{P}_{\rm sig}(m_{\rm ES})$, $\mathcal{P}_{{\rm sig},B\overline{B}}(\Delta E)$, and the sharper structures in $\mathcal{P}_{B\overline{B}}(m_{\rm ES})$ and $\mathcal{P}_j(m_k)$; linear or quadratic dependences for combinatorial components of $\mathcal{P}_{B\overline{B},q\overline{q}}(m_k)$ and for $\mathcal{P}_{q\overline{q}}(\Delta E)$; quadratic functions for $\mathcal{P}_j(|\mathcal{H}_\omega|)$ and $\mathcal{P}_j(\mathcal{H}_{\rho^+})$; and a Gaussian of different widths below and above the peak, plus a broad Gaussian, for $\mathcal{P}_j(\mathcal{F})$. The $q\overline{q}$ background in $m_{\rm ES}$ is described by the function $x\sqrt{1-x^2}\exp\left[-\xi(1-x^2)\right]$, with $x \equiv 2m_{\rm ES}/\sqrt{s}$ and parameter ξ. These are discussed in more detail in Ref. [23] and can be seen in Fig. 1 for the $B^+ \to \eta\rho^+$ decay.

We allow the parameters most important for the determination of the combinatorial background PDFs to

TABLE II: Number of events N in the sample, fitted signal yield Y_S in events (ev.) with statistical error, measured bias, detection efficiency ϵ, daughter branching fraction product ($\prod \mathcal{B}_i$), and measured branching fraction $\mathcal{B}$ with statistical error for each decay chain, and the measured charge asymmetry $\mathcal{A}_{ch}$ for the decay $B^+ \rightarrow \eta\rho^+$. For the combined measurements the significance $\mathcal{S}$ (with systematic uncertainties included), branching fraction with statistical and systematic error, and in parentheses the 90% C.L. upper limits.

Mode	N (ev.)	Y_S (ev.)	Bias (ev.)	ϵ (%)	$\prod \mathcal{B}_i$ (%)	$\mathcal{S}$ (σ)	$\mathcal{B}$ (10^{-6})	$\mathcal{A}_{ch}$
$\boldsymbol{\eta\rho^+}$						**9.0**	$\mathbf{9.9 \pm 1.2 \pm 0.8}$	$\mathbf{0.13 \pm 0.11 \pm 0.02}$
$\eta_{\gamma\gamma}\rho^+$	104609	326^{+44}_{-42}	17 ± 9	16.7	39.4		10.2 ± 1.4	0.07 ± 0.12
$\eta_{3\pi}\rho^+$	47918	123^{+27}_{-26}	13 ± 7	11.7	22.6		9.1 ± 2.2	0.28 ± 0.21
$\boldsymbol{\eta'\eta}$						**1.4**	$\mathbf{0.5 \pm 0.4 \pm 0.1}$ (<**1.2**)	
$\eta'_{\eta\pi\pi}\eta_{\gamma\gamma}$	2191	$8.8^{+6.4}_{-5.1}$	0.9 ± 0.5	25.6	6.9		$1.0^{+0.8}_{-0.6}$	
$\eta'_{\eta\pi\pi}\eta_{3\pi}$	896	$3.2^{+5.1}_{-4.1}$	0.2 ± 0.2	16.7	4.0		$1.0^{+1.7}_{-1.4}$	
$\eta'_{\rho\gamma}\eta_{\gamma\gamma}$	39723	$0.7^{+12.2}_{-8.6}$	0.0 ± 0.5	25.6	11.6		$0.1^{+0.7}_{-0.6}$	
$\eta'_{\rho\gamma}\eta_{3\pi}$	20672	$0.7^{+9.4}_{-6.8}$	2.0 ± 1.0	18.2	6.7		$-0.2^{+1.7}_{-1.2}$	
$\boldsymbol{\eta\pi^0}$						**2.2**	$\mathbf{0.9 \pm 0.4 \pm 0.1}$ (<**1.5**)	
$\eta_{\gamma\gamma}\pi^0$	9085	$18.6^{+23.9}_{-21.7}$	4.4 ± 2.2	20.5	39.4		0.4 ± 0.6	
$\eta_{3\pi}\pi^0$	4030	$23.3^{+12.5}_{-11.1}$	1.7 ± 0.9	17.3	22.6		$1.3^{+0.7}_{-0.6}$	
$\boldsymbol{\eta'\pi^0}$						**3.1**	$\mathbf{0.9 \pm 0.4 \pm 0.1}$ (<**1.5**)	
$\eta'_{\eta\pi\pi}\pi^0$	3784	$20.6^{+9.4}_{-8.0}$	1.8 ± 0.9	22.5	17.5		$1.1^{+0.5}_{-0.4}$	
$\eta'_{\rho\gamma}\pi^0$	19789	$12.2^{+18.4}_{-16.3}$	2.7 ± 1.4	18.9	29.5		$0.4^{+0.7}_{-0.6}$	
$\boldsymbol{\omega\pi^0}$	39822	$2.4^{+19.9}_{-16.8}$	0.5 ± 0.5	18.4	89.1	**0.3**	$\mathbf{0.07 \pm 0.26 \pm 0.02}$ (<**0.5**)	

vary in the fit, along with the yields for all components. Specifically, the free background parameters are most or all of the following, depending on the decay mode: ξ for $m_{\rm ES}$, linear and quadratic coefficients for ΔE, area and slope of the combinatorial component for m_k, and the mean, width, and width difference parameters for $\mathcal{F}$. Results for the signal yields are presented in the third column of Table II for each sample.

We test and calibrate the fitting procedure by applying it to ensembles of simulated experiments composed of $q\overline{q}$ events drawn from the PDF, into which we have embedded the expected number of signal and charmless $B\overline{B}$ background events randomly extracted from the fully simulated MC samples. We find biases of 0–17 events, somewhat dependent on the signal yield. The bias values obtained for simulations that reproduce the yields found in the data are given in the fourth column of Table II. Figure 1 shows PDFs and projections of subsamples of the data, enriched with a threshold requirement on the signal likelihood (computed without the variable plotted) for the $B^+ \rightarrow \eta\rho^+$ decay. Figure 2 shows projections for the other four modes.

We determine the reconstruction efficiencies, given in Table II, as the ratio of reconstructed and accepted events in simulation to the number generated. We compute the branching fraction for each channel by subtracting the fit bias from the measured yield, and dividing the result by the efficiency and the number of produced $B\overline{B}$ pairs [23]. We assume that the branching fractions of the $\Upsilon(4S)$ to B^+B^- and $B^0\overline{B}^0$ are each equal to 50%. Table II gives the numbers pertinent to these computations.

We combine results where we have multiple decay channels by adding for each channel the function $-2\ln\{[\mathcal{L}(\mathcal{B})/\mathcal{L}(\mathcal{B}_0)] \otimes G(\mathcal{B};0,\sigma')\}$, where $\mathcal{B}_0$ is the central value from the fit, σ' is the part of the systematic uncertainty uncorrelated with other channels, and $\otimes G$ denotes convolution with a Gaussian function; the part of the systematic uncertainty common to all channels is then added in quadrature. We give the resulting final branching fractions for each mode in Table II with the significance, taken as the square root of the difference between the value of $-2\ln\mathcal{L}(\mathcal{B})$ (with only additive systematic uncertainties included) for zero signal and the value at its minimum. The 90% confidence level (C.L.) upper limits are taken to be the branching fraction below which lies 90% of the total of the likelihood integral in the positive branching fraction region.

The systematic uncertainties on the branching fractions arising from lack of knowledge of the PDFs have been included in part in the statistical error since most background parameters are free in the fit. For the signal, the uncertainties in PDF parameters are estimated from the consistency of fits to MC and data in control modes. Varying the signal-PDF parameters within these errors, we estimate yield uncertainties of 0.3–7 events, depending on the decay mode. The uncertainty from fit bias (Table II) includes the statistical uncertainty from the simulated experiments added in quadrature with one-half of the fit-bias correction. We estimate the uncertainty from modeling the charmless $B\overline{B}$ backgrounds by accounting for the uncertainties in the knowledge of their branching fractions. These additive errors are the largest systematic errors for the modes with small signal yield (but not $B^+ \rightarrow \eta\rho^+$).

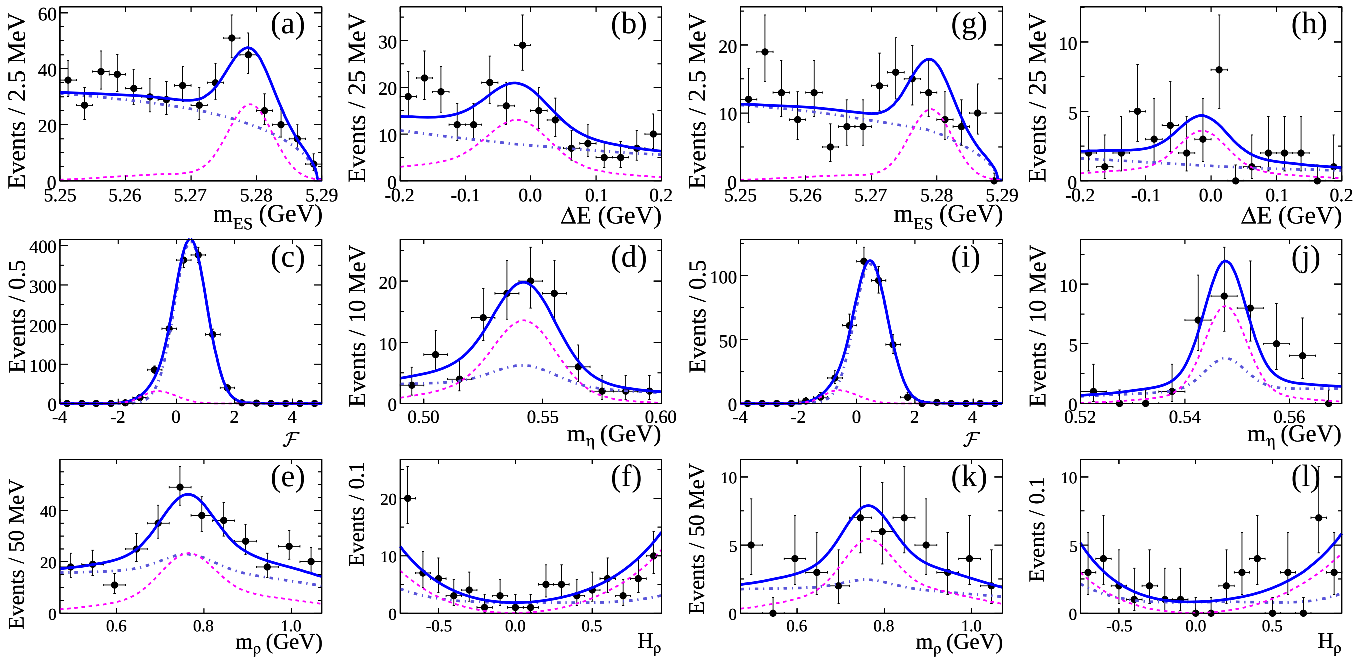

FIG. 1: Signal-enhanced projections for $\eta_{\gamma\gamma}\rho^+$ (left) and $\eta_{3\pi}\rho^+$ (right) for (a,g) $m_{\rm ES}$, (b,h) ΔE, (c,i) $\mathcal{F}$, (d,j) m_η, (e,k) m_ρ, (f,l) $\mathcal{H}_\rho$. The total ($q\overline{q}$ plus $B\overline{B}$) background fit function is shown as blue dot-dashed, signal as magenta dashed, and the total as a solid blue line. These plots are made with a minimum requirement on the likelihood that has an efficiency for signal of 15–35% while reducing the background by between two and three orders of magnitude.

Uncertainties in our knowledge of the efficiency, found from auxiliary studies, include $0.4\% \times N_t$ and $1.5\% \times N_\gamma$, where N_t and N_γ are the number of tracks and photons, respectively, in the B candidate. The uncertainty in the total number of $B\overline{B}$ pairs in the data sample is 1.1%. Published data [20] provide the uncertainties in the B-daughter product branching fractions (0.7–3.9%). The uncertainties in the efficiency from the event selection are about 0.5%.

We observe the decay $B^+ \rightarrow \eta\rho^+$ with a significance of 9 standard deviations. The branching fraction $(9.9 \pm 1.2 \pm 0.8) \times 10^{-6}$ and charge asymmetry $0.13 \pm 0.11 \pm 0.02$ are in good agreement with the theoretical expectations. We do not find evidence for the other four decays though the sensitivity of these measurements is now comparable to the range of the theoretical estimates.

We are grateful for the excellent luminosity and machine conditions provided by our PEP-II colleagues, and for the substantial dedicated effort from the computing organizations that support *BABAR*. The collaborating institutions wish to thank SLAC for its support and kind hospitality. This work is supported by DOE and NSF (USA), NSERC (Canada), CEA and CNRS-IN2P3 (France), BMBF and DFG (Germany), INFN (Italy), FOM (The Netherlands), NFR (Norway), MES (Russia), MEC (Spain), and STFC (United Kingdom). Individuals have received support from the Marie Curie EIF (European Union) and the A. P. Sloan Foundation.

---

[*] Deceased

[†] Now at Temple University, Philadelphia, Pennsylvania 19122, USA

[‡] Now at Tel Aviv University, Tel Aviv, 69978, Israel

[§] Also with Università di Perugia, Dipartimento di Fisica, Perugia, Italy

[¶] Also with Università di Sassari, Sassari, Italy

[1] M. Beneke and M. Neubert, Nucl. Phys. B **675**, 333 (2003) and references therein.

[2] M.-Z. Yang and Y.-D. Yang, Nucl. Phys. B **609**, 469 (2001); M. Beneke and M. Neubert, Nucl. Phys. B **651**, 225 (2003);

[3] H. K. Fu *et al.*, Phys. Rev. D **69**, 074002 (2004).

[4] C.-W. Chiang *et al.*, Phys. Rev. D **70**, 034020 (2004); C.-W. Chiang and Y.-F. Zhou, JHEP **12**, 27 (2006).

[5] C.-W. Chiang, M. Gronau, and J. L. Rosner, Phys. Rev. D **68**, 074012 (2003); C.-W. Chiang *et al.*, Phys. Rev. D **69**, 034001 (2004).

[6] H. Wang *et al.*, Nucl. Phys. B **738**, 243 (2006).

[7] A. R. Williamson and J. Zupan, Phys. Rev. D **74**, 014003 (2006).

[8] *BABAR* Collaboration, B. Aubert *et al.*, Phys. Rev. Lett. **95**, 131803 (2005).

[9] *BABAR* Collaboration, B. Aubert *et al.*, Phys. Rev. D **70**, 032006 (2004); *BABAR* Collaboration, B. Aubert *et al.*, Phys. Rev. D **73**, 071102 (2006).

[10] Belle Collaboration, P. Chang *et al.*, Phys. Rev. D **71**, 091106 (2005); Belle Collaboration, J. Schümann *et al.*, Phys. Rev. Lett. **97**, 061802 (2006); Belle Collaboration, J. Schümann, C.H. Wang *et al.*, Phys. Rev. D **75**, 092002

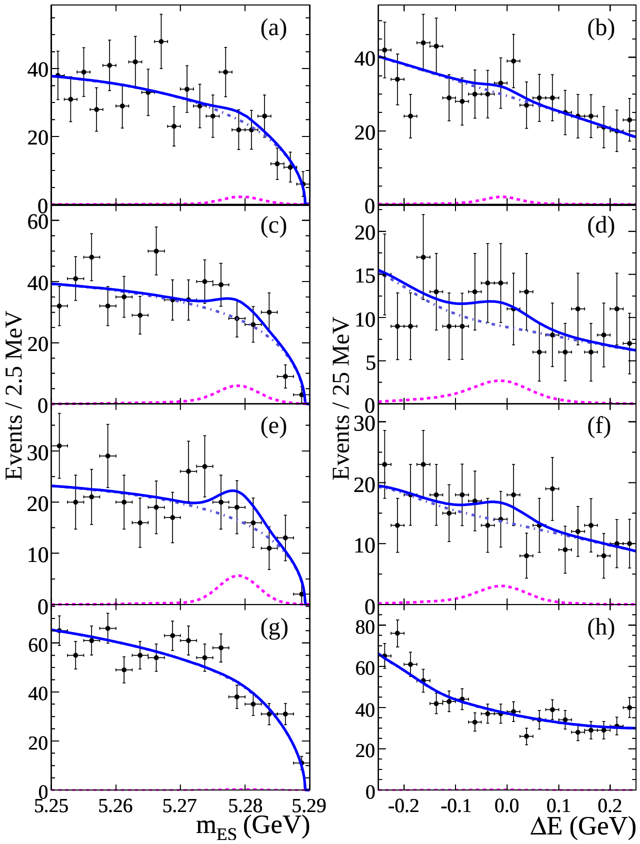

FIG. 2: Signal-enhanced projections of the B^0-candidate $m_{\rm ES}$ and ΔE mass for (a, b) $B^0 \to \eta'\eta$, (c, d) $B^0 \to \eta\pi^0$, (e, f) $B^0 \to \eta'\pi^0$, and (g, h) $B^0 \to \omega\pi^0$. Points with errors represent data, solid curves the full fit functions (both signal modes combined), dot-dashed curves the background functions (the peaking $B\overline{B}$ background component is small), and dashed curve the fit signal function. These plots are made with a minimum requirement on the likelihood that has an efficiency for signal of 45–75%.

(2007); Belle Collaboration, C. H. Wang *et al.*, Phys. Rev. D **75**, 092005 (2007).

[11] CLEO Collaboration, B. H. Behrens *et al.*, Phys. Rev. Lett. **80**, 3710 (1998); CLEO Collaboration, S. J. Richichi *et al.*, Phys. Rev. Lett. **85**, 520 (2000); CLEO Collaboration, C. P. Jessop *et al.*, Phys. Rev. Lett. **85**, 2881 (2000).

[12] Y. Grossman, *et al.*, Phys. Rev. D **68**, 015004 (2003).

[13] M. Gronau, J.L. Rosner and J. Zupan, Phys. Rev. D **74**, 093003 (2006).

[14] Belle Collaboration, K.-F. Chen *et al.*, Phys. Rev. Lett. **98**, 072003 (2007); *BABAR* Collaboration, B. Aubert *et al.*, Phys. Rev. Lett. **99**, 171803 (2007).

[15] M. Beneke, Phys. Lett. B **620**, 143 (2005).

[16] M. Gronau and J. Zupan, Phys. Rev. D **71**, 074017 (2005).

[17] S. Gardner, Phys. Rev. D **72**, 034015 (2005).

[18] *BABAR* Collaboration, B. Aubert *et al.*, Nucl. Instrum. Methods Phys. Res., Sect. A **479**, 1 (2002).

[19] The *BABAR* detector Monte Carlo simulation is based on GEANT4 [S. Agostinelli *et al.*, Nucl. Instrum. Methods Phys. Res., Sect. A **506**, 250 (2003)] and EvtGen [D. J. Lange, Nucl. Instrum. Methods Phys. Res., Sect. A **462**, 152 (2001)].

[20] Particle Data Group, Y.-M. Yao *et al.*, J. Phys. **G33**, 1 (2006).

[21] *BABAR* Collaboration, B. Aubert *et al.*, Phys. Rev. D **74**, 011106 (2006).

[22] *BABAR* Collaboration, B. Aubert *et al.*, Phys. Rev. Lett. **99**, 171803 (2007).

[23] *BABAR* Collaboration, B. Aubert *et al.*, Phys. Rev. D **70**, 032006 (2004).